Supplemental Materials

Advanced Thermoelectrics Governed by Single Parabolic Band Model:

$Mg_2Si_{0.3}Sn_{0.7}$, a Canonical Example

Wei Liu[1, 2]†, Hang Chi[1]†, Hui Sun[1], Qiang Zhang[2], Kang Yin[2],

Xinfeng Tang[2]*, Qingjie Zhang[2] and Ctirad Uher[1]*

[1]Department of Physics, University of Michigan, Ann Arbor, Michigan 48109, USA
[2]State Key Laboratory of Advanced Technology for Materials Synthesis and Processing,
Wuhan University of Technology, Wuhan 430070, China

*Correspondence email(s): C.U., cuher@umich.edu, X.T., tangxf@whut.edu.cn.

†These authors contributed equally to this work.

In the Single Parabolic Band (SPB) model, with an energy dependent relaxation time

$$\tau = \tau_0 \varepsilon^r,$$ (S1)

all transport coefficients can be obtained by solving the Boltzmann transport equation [1-3]. Specifically, the Seebeck coefficient is given by

$$S = -\frac{k_B}{q}\left[\eta - \frac{\left(r+\frac{5}{2}\right)F_{r+\frac{3}{2}}(\eta)}{\left(r+\frac{3}{2}\right)F_{r+\frac{1}{2}}(\eta)}\right],$$ (S2)

where k_B is the Boltzmann constant, $q = -e$ is the electron charge, η $(=E_F/k_BT)$ is the reduced Fermi level measured from the conduction band minimum, $r = -1/2$ for any scattering mechanism whose mean-free path ℓ is independent of energy (MFPIE), such as acoustic phonon (AP) scattering and alloy scattering (AS) found relevant in this research, and $F_n(\eta)$ is the Fermi integral given by:

$$F_n(\eta) = \int_0^\infty \frac{1}{e^{\xi-\eta}+1}\xi^n d\xi.$$ (S3)

The experimentally accessible n_H $(= 1/qR_H$, where R_H is the Hall coefficient) is related to the free carrier density n via the Hall factor r_H:

$$n_H = n/r_H,$$ (S4)

where

$$r_H = \frac{3}{2}\frac{\left(2r+\frac{3}{2}\right)}{\left(r+\frac{3}{2}\right)^2}\frac{F_{2r+\frac{1}{2}}(\eta)F_{\frac{1}{2}}(\eta)}{F_{r+\frac{1}{2}}^2(\eta)},$$ (S5)

and

$$n = \frac{4\pi\left(2m^* k_B T\right)^{3/2}}{h^3} F_{\frac{1}{2}}(\eta).$$ (S6)

Here m^* is the density-of-states effective mass given as a function of the single valley effective mass m_s^* and the associated valley degeneracy N_v as

$$m^* = N_v^{2/3} m_s^*.$$ (S7)

Considering only the dominant scattering mechanisms of AP and AS, the overall μ_H is given by the Matthiessen's rule

$$\frac{1}{\mu_H} = \frac{1}{\mu_H^{AS}} + \frac{1}{\mu_H^{AP}}.$$ (S8)

Noting that

$$\mu_H^s = \mu_{d,0}^s \Psi_r(\eta),$$ (S9)

where $\Psi_r(\pi)$ is given by

$$\Psi_r(\eta) = \frac{3\sqrt{\pi}}{4} \frac{2r + \frac{3}{2}}{r + \frac{3}{2}} \frac{1}{\Gamma\left(r + \frac{5}{2}\right)} \frac{F_{2r+\frac{1}{2}}(\eta)}{F_{r+\frac{1}{2}}(\eta)},$$ (S10)

with s (= AS, AP) indicating different scattering mechanisms. $\mu_{d,0}^s$ represents the drift mobility in the non-degenerate limit which can be calculated, for the MFPIE case, with the knowledge of the corresponding mean-free path $\ell_{d,0}^{MFPIE}$ from

$$\mu_{d,0}^{MFPIE} = \frac{4}{3} \frac{q\ell_{d,0}^{MFPIE}}{\left(2\pi m_s^* k_B T\right)^{1/2}}$$ (S11)

The literature result[4] for AS is

$$\mu_{d,0}^{AS} = \frac{64e\hbar^4 N_0}{9(2\pi)^{3/2} x(1-x) E_a^2 \left(m_s^*\right)^{5/2} \left(k_B T\right)^{1/2}},$$ (S12)

where x (= 0.7 for $Mg_2Si_{0.3}Sn_{0.7}$) is the Sn fraction in the solid solution, N_0 is the number of atoms per unit volume, and E_a is the parameter characterizing the alloy potential fluctuation in $Mg_2Si_{0.3}Sn_{0.7}$. The result for AP is[5]

$$\mu_{d,0}^{AP} = \frac{(8\pi)^{1/2} e\hbar^4 \rho v_l^2}{3E_d^2 (m_s^*)^{5/2} (k_B T)^{3/2}}$$
(S13)

where v_l is the longitudinal velocity of sound and ρ is the density. E_d is the deformation potential.

The electronic thermal conductivity κ_e can be determined by using the Wiedemann-Franz law, $\kappa_e = L\sigma T$, where L is the Lorenz number, σ is the electrical conductivity and T the absolute temperature. L and its temperature dependence are given by[6]

$$L = \left(\frac{k_B}{q}\right)^2 \left\{ \frac{\left(r+\frac{7}{2}\right)F_{r+\frac{5}{2}}(\eta)}{\left(r+\frac{3}{2}\right)F_{r+\frac{1}{2}}(\eta)} - \left[\frac{\left(r+\frac{5}{2}\right)F_{r+\frac{3}{2}}(\eta)}{\left(r+\frac{3}{2}\right)F_{r+\frac{1}{2}}(\eta)} \right]^2 \right\}$$
(S14)

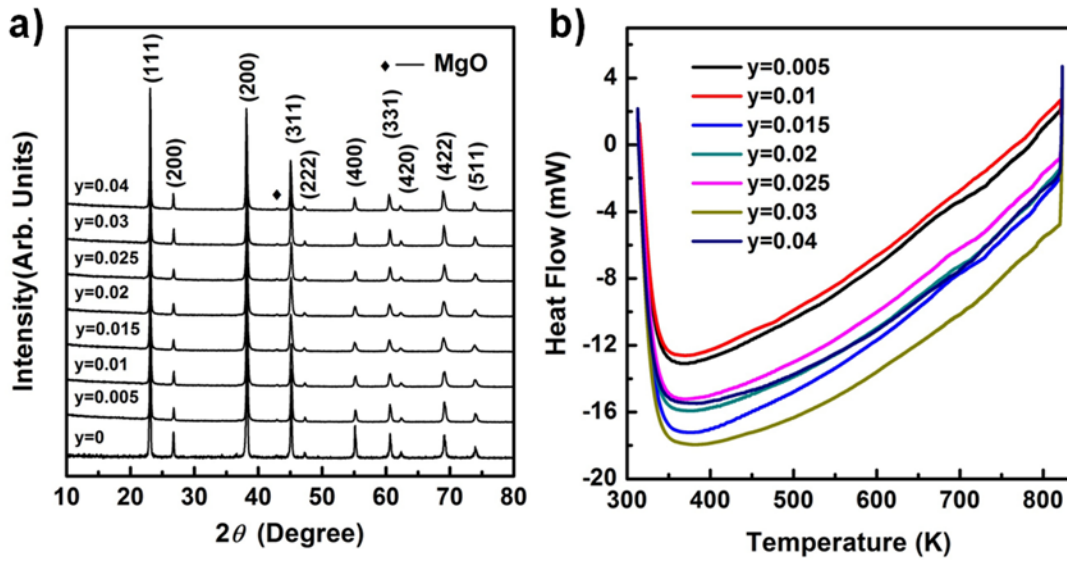Figure S1: (a) XRD patterns and (b) DSC curves of $Mg_2(Si_{0.3}Sn_{0.7})_{1-y}Bi_y$ ($0 \leq y \leq 0.04$) solid solutions. Results indicate that, similar to the other $Mg_2Si_{1-x}Sn_x$-based solid solutions,[7-10] all XRD patterns of $Mg_2(Si_{0.3}Sn_{0.7})_{1-y}Bi_y$ can be indexed to the $Mg_2Si_{0.3}Sn_{0.7}$ solid solution with the cubic structure and space group of Fm3m, except for one slight peak belonging to MgO. In addition, DSC curves evolve gradually with temperature in the range of 350-820 K and no anomalous thermal effects are observed, attesting to $Mg_2(Si_{0.3}Sn_{0.7})_{1-y}Bi_y$ being stable during measurements.
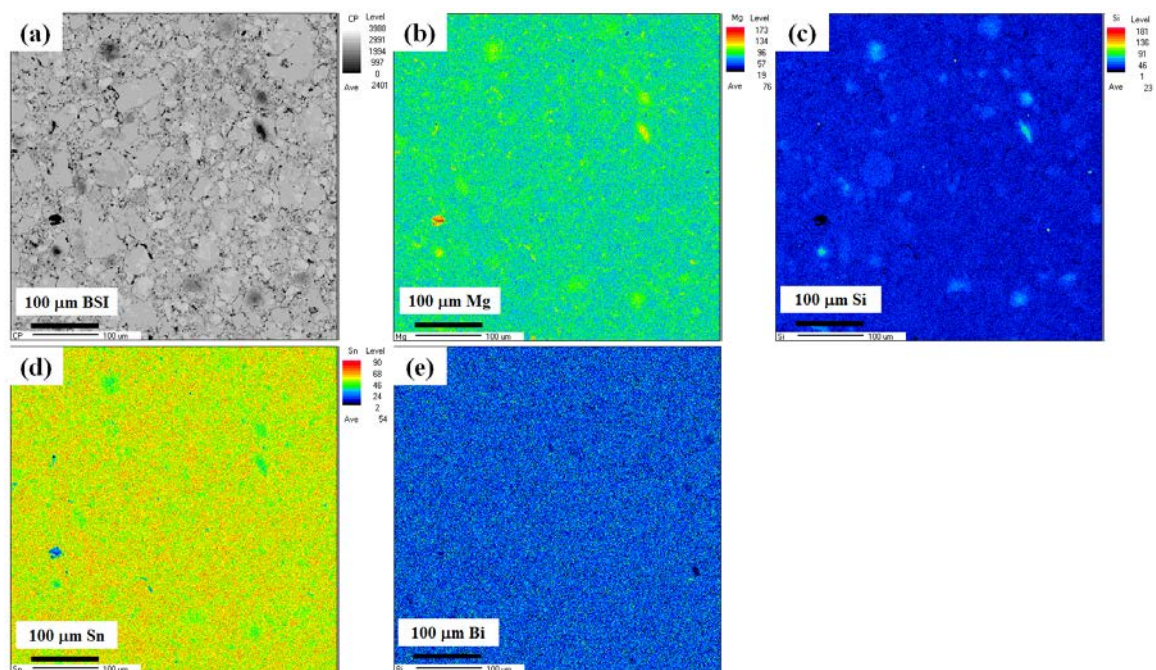
Figure S2: Back Scattering Image (a), elemental mapping distribution of Mg (b), Si (c), Sn (d) and Bi (e) for $Mg_2(Si_{0.3}Sn_{0.7})_{0.97}Bi_{0.03}$. All the constituent elements distribute rather evenly in the micron size scale. We should note that, even Bi doping amount is as high as $y = 0.03$, we do not observe obvious segregation in the matrix of $Mg_2(Si_{0.3}Sn_{0.7})_{0.97}Bi_{0.03}$.
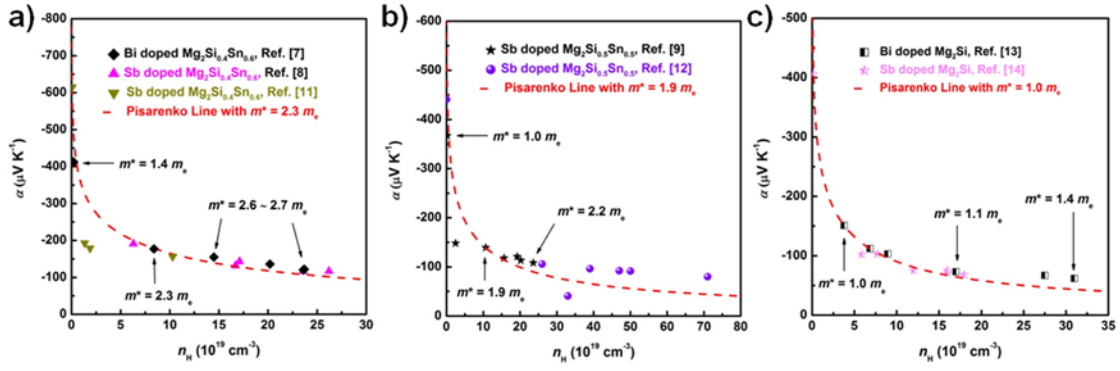
Figure S3: (a) correlation between the Seebeck coefficient S and the Hall carrier density n_H at room temperature for $Mg_2Si_{0.4}Sn_{0.6}$ (b), $Mg_2Si_{0.5}Sn_{0.5}$ (b), and Mg_2Si (c), respectively.[7-9, 11-14]. The single parabolic band (SPB) model is utilized to generate the density-of-states effective mass m^* from S and n_H. The closer the composition of $Mg_2Si_{1-x}Sn_x$ to the band convergence at $Mg_2Si_{0.3}Sn_{0.7}$, the better is the coincidence between the experimental S and the Pisarenko curve based on the SPB model, especially when $n_H > 8.4 \times 10^{19}$ cm^{-3}.

1. E. H. Putley, *The Hall Effect and Related Phenomena*, Butterworths, London, 1960.

2. H. J. Goldsmid, *Electronic Regrigeration*, Pion, London, 1985.

3. A. F. May, E. S. Toberer, A. Saramat and G. J. Snyder, *Phys. Rev. B*, 2009, **80**.

4. J. W. Harrison and J. R. Hauser, *Phys. Rev. B*, 1976, **13**, 5347-5350.

5. J. Bardeen and W. Shockley, *Phys. Rev.*, 1950, **80**, 72-80.

6. H. J. Goldsmid, *Electronic Refrigeration*, Pion, London, 1986.

7. W. Liu, Q. Zhang, K. Yin, H. Chi, X. Zhou, X. Tang and C. Uher, *J Solid State Chem*, 2013, **203**, 333-339.

8. W. Liu, X. Tang, H. Li, K. Yin, J. Sharp, X. Zhou and C. Uher, *J. Mater. Chem.*, 2012, **22**, 13653-13661.

9. W. Liu, X. Tang, H. Li, J. Sharp, X. Zhou and C. Uher, *Chem. Mater.*, 2011, **23**, 5256-5263.

10. W. Liu, X. Tang and J. Sharp, *Journal of Physics D: Applied Physics*, 2010, **43**, 085406.

11. Q. Zhang, J. He, T. J. Zhu, S. N. Zhang, X. B. Zhao and T. M. Tritt, *Appl. Phys. Lett.*, 2008, **93**, 102109-102103.

12. H. Gao, T. Zhu, X. Liu, L. Chen and X. Zhao, *J. Mater. Chem.*, 2011, **21**, 5933-5937.

13. S. K. Bux, M. T. Yeung, E. S. Toberer, G. J. Snyder, R. B. Kaner and J.-P. Fleurial, *J. Mater. Chem.*, 2011, **21**, 12259-12266.

14. G. S. Nolas, D. Wang and M. Beekman, *Phys. Rev. B*, 2007, **76**, 235204.